



Article

Sustainable Algae-Derived Carbon Particles from Hydrothermal Liquefaction: An Innovative Reinforcing Agent for Epoxy Matrix Composite

Abhijeet Mali ¹, Philip Agbo ¹, Shobha Mantripragada ¹, Vishwas S. Jadhav ¹, Lijun Wang ^{2,*} and Lifeng Zhang ^{1,*}

- Department of Nanoengineering, Joint School of Nanoscience and Nanoengineering, North Carolina A&T State University, 2907 East Gate City Boulevard, Greensboro, NC 27401, USA
- Department of Natural Resources and Environmental Design, College of Agriculture and Environmental Sciences, North Carolina A&T State University, 1601 East Market Street, Greensboro, NC 27411, USA
- * Correspondence: lwang@ncat.edu (L.W.); lzhang@ncat.edu (L.Z.); Tel.: +1-336-285-3833 (L.W.); +1-336-285-2875 (L.Z.)

Abstract: Algae is a promising sustainable feedstock for the generation of bio-crude oil, which is a sustainable alternative to fossil fuels, through the thermochemical process of hydrothermal liquefaction (HTL). However, this process also generates carbon particles (algae-derived carbon, ADC) as a significant byproduct. Herein, we report a brand-new and value-added use of ADC particles as a reinforcing agent for epoxy matrix composites (EMCs). ADC particles were synthesized through HTL processing of Chlorella vulgaris (a green microalgae) and characterized for morphology, average size, specific surface area, porosity, and functional groups. The ADC particles were subsequently integrated into a representative epoxy resin (EPON 862) as a reinforcing filler at loading levels of 0.25%, 0.5%, 1%, and 2% by weight. The tensile, flexural, and Izod impact properties, as well as the thermal stability, of the resulting EMCs were evaluated. It is revealed that the ADC particles are a sustainable and effective reinforcing agent for EMCs at ultra-low loading. Specifically, the ADC-reinforced EMC with 1 wt.% ADC showed improvements of ~24%, ~30%, ~31%, and ~57% in tensile strength, Young's modulus, elongation at break, and work of fracture (WOF), respectively, and improvements of ~10%, ~37%, ~24%, and ~39% in flexural strength, flexural modulus, flexural elongation at break, and flexural WOF, respectively, as well as an improvement of ~54% in Izod impact strength, compared to those corresponding properties of neat epoxy. In the meantime, the thermal decomposition temperatures at 60% and 80% weight loss of the abovementioned ADC-reinforced EMC increased from 410 °C to 415 °C and from 448 °C to 515 °C in comparison with those of neat epoxy. This study highlighted the potential of sustainable ADC particles as a reinforcing agent in the field of polymer matrix composite materials, which represented a novel and sustainable approach that would mitigate greenhouse gas remission and reduce reliance on nonrenewable reinforcing fillers in the polymer composite industry.

Keywords: microalgae; hydrothermal liquefaction; carbon particle; reinforcing effect; epoxy composite



Citation: Mali, A.; Agbo, P.; Mantripragada, S.; Jadhav, V.S.; Wang, L.; Zhang, L. Sustainable Algae-Derived Carbon Particles from Hydrothermal Liquefaction: An Innovative Reinforcing Agent for Epoxy Matrix Composite. Sustainability 2024, 16, 6870. https:// doi.org/10.3390/su16166870

Academic Editor: Giovanni Leonardi

Received: 23 July 2024 Revised: 5 August 2024 Accepted: 8 August 2024 Published: 10 August 2024



Copyright: © 2024 by the authors. Licensee MDPI, Basel, Switzerland. This article is an open access article distributed under the terms and conditions of the Creative Commons Attribution (CC BY) license (https://creativecommons.org/licenses/by/4.0/).

1. Introduction

Epoxy resin is a popular thermosetting polymer and has gained great attention in many industries and applications over the past years [1–3]. Epoxy resin alone, however, is inherently brittle and susceptible to cracking and thus cannot provide comprehensive mechanical properties when it is used as a matrix in composite materials. Therefore, it is crucial to reinforce epoxy resin to achieve comprehensive mechanical performance in the resultant epoxy matrix composites (EMCs) [4,5]. Various reinforcing fillers including fibers and particles are employed to enhance the mechanical performance of EMCs and make

Sustainability **2024**, 16, 6870 2 of 14

them more advantageous in extensive applications such as automotive, aerospace, and sporting goods [6–8].

Rigid particles are an important reinforcing filler for high performance EMCs. Strengthening EMCs through rigid particles typically involves multiple mechanisms such as load transfer, crack path deflection, micro cracking, and stress redistribution, which collectively contribute to improving the overall mechanical performance of EMCs [9,10]. Researchers have attempted to improve the mechanical performance of EMCs using glass, alumina, dolomite [11,12], titanium dioxide [13], silicon carbide [14], and metal particles [15]. Considering the environmental impact and sustainable development, there is a need to develop sustainable and environmentally friendly reinforcing fillers for EMCs without compromising their performance.

Biochar is a carbon solid and generally prepared through thermochemical processing of biomass such as pyrolysis and hydrothermal carbonization. Biochar has attracted attention in polymer composite materials due to its porous structure and large specific surface area, as well as its renewability and cost-effectiveness [16]. Biochar produced from waste biomass feedstock like rice husk, pine wood waste, cassava, durian peel, corncob, arhar stalks, willows, wheat straw, etc., has been proven to be a significant member of particle fillers in improving thermal and mechanical properties of polymer matrix composites [17–21].

Hydrothermal liquefaction (HTL) is a thermochemical process using water as a medium that converts biomass into bio-crude oil under moderate temperature and high pressure [22]. Algae stand out as an exceptional feedstock for HTL production of bio-crude oil due to its rapid growth rate in various aquatic conditions, and environmental benefits like waste reduction, water purification, and high greenhouse gas fixation efficiency [23–25]. It is worth noting that carbon residue is invariably produced as a byproduct in the HTL processing of algae, which is similar to the biochar (also termed as hydrochar) produced by hydrothermal carbonization of biomass. Although investigations have delved into incorporating the biochar into polymer composites, research on the reinforcing effect of the carbon particle byproduct from HTL processing of microalgae (termed as algae-derived carbon (ADC) herein) in polymer composites is not yet addressed. The ADC particles may serve as a potential particle filler for high-performance polymer composites.

For the first time, this research evaluated sustainable ADC particles, a byproduct from the HTL processing of microalgae, as a reinforcing agent in EMCs. The ADC particles were incorporated at various loadings including 0.25%, 0.5%, 1%, and 2% by weight to assess the mechanical performance of the resulting ADC-reinforced EMCs including tensile, flexural, and impact properties. Moreover, thermal stability of the ADC-reinforced EMCs was also studied by thermogravimetric analysis (TGA). The findings from this research provided insights into the reinforcing effects of ADC particles on EMCs, which is an innovative strategy that meets the demand for environmentally friendly sustainable reinforcing fillers and effective waste management in development of high-performance EMC materials.

2. Materials and Methods

2.1. Materials

A green microalga, *Chlorella vulgaris*, was acquired from Nuts.com (Cranford, NJ, USA) to synthesize ADC particles. A phenol-formaldehyde polymer glycidyl ether type epoxy resin (EPON 862) and its curing agent (EPIKURE W) were procured from Miller Stephenson (Danbury, CT, USA). Ethanol and anhydrous acetone were purchased from Fisher Scientific (Waltham, MA, USA). All chemicals were utilized in their original state without additional purification.

2.2. Preparation of ADC Particles

ADC particles were prepared from hydrothermal liquefaction (HTL) processing of *Chlorella vulgaris* (Figure 1).

Sustainability **2024**, 16, 6870 3 of 14

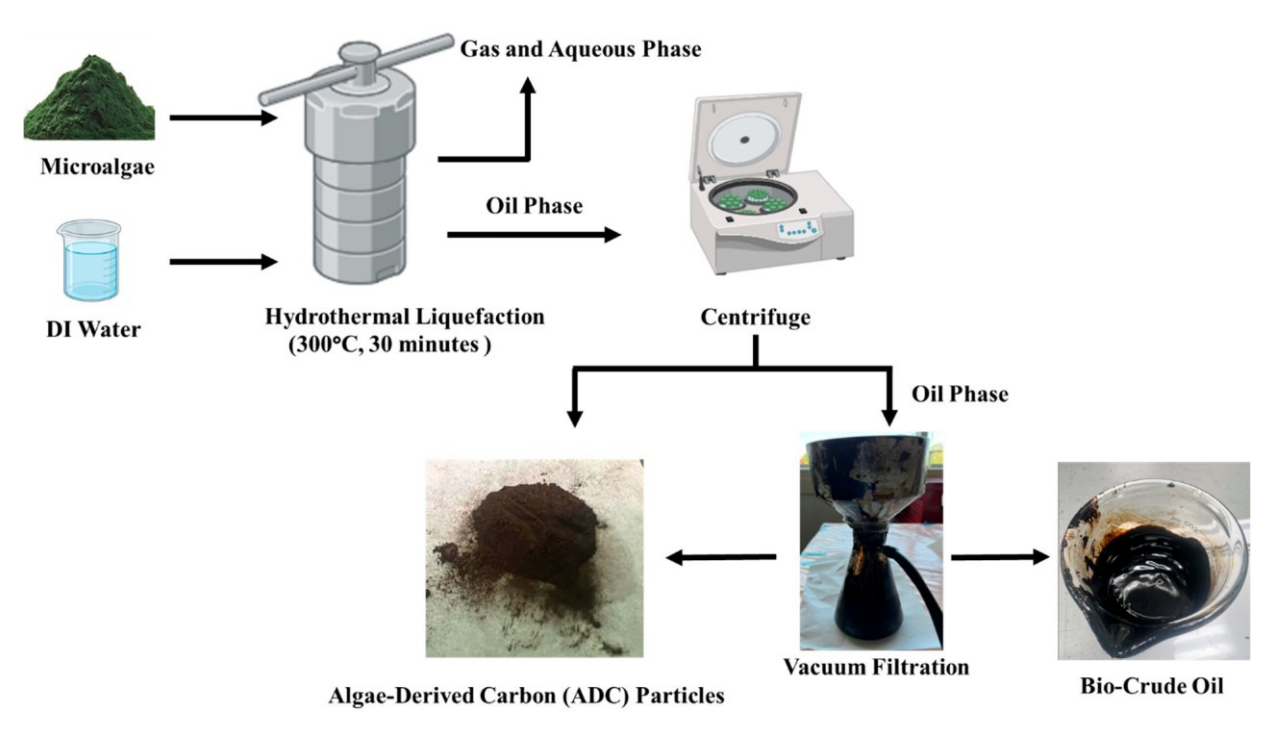


Figure 1. Schematic diagram for ADC particle preparation.

Specifically, a PARR reactor (model 4570, Parr Instrument Company, Moline, IL, USA) of 1-L capacity was used for the HTL process. The reactor was loaded with deionized water and algae in a ratio of 9.6:1 [26]. The reactor was heated from room temperature to 300 °C with a heating rate of 5 °C/min. The HTL reaction was conducted with a residence time of 30 min under a pressure of 1500 psi. After the reaction was completed, the PARR reactor was rapidly quenched to room temperature using an internal cooling water coil, and then off-gas was vented to bring down the pressure in the reactor back to atmospheric level. The HTL products consisted of an oily residue phase and an aqueous phase. The residue phase contained both bio-crude oil and ADC particles. The bio-crude oil was extracted using acetone followed by centrifugation at 4000 rpm for 15 min and subsequent vacuum filtration. The remaining ADC particles were thoroughly washed three times with acetone and then centrifuged to remove any leftover bio-crude oil. The obtained ADC particles were dried in an oven at 80 °C for 8 h.

2.3. Fabrication of ADC-Reinforced Epoxy Matrix Composites (EMCs)

Prior to incorporating ADC particles as a reinforcing agent in EMCs, the ADC particles were sonicated using a 500 W ultrasonic probe sonicator (QSONICA, Newtown, CT, USA) at 80% power for a duration of 30 min in acetone with the intention to break agglomeration and reduce the size of ADC particles. After sonication, the ADC particles were subjected to centrifugation followed by drying in an oven at 80 $^{\circ}$ C for 8 h.

ADC particles were used as a reinforcing agent to make EMCs with ADC loadings at 0.25 wt.%, 0.5 wt.%, 1 wt.%, and 2 wt.%, respectively. Initially, the epoxy resin was heated and degassed in an oven under vacuum at 60 °C for 10 min. Next, ADC particles were added to the epoxy resin at corresponding loadings. The resultant mixture was further subjected to vigorous ultrasonication using the ultrasonic probe sonicator at 40% power for 10 min to acquire homogeneous dispersion of ADC particles in the epoxy matrix. The curing agent was then added into the epoxy system at 26.4 wt.% of epoxy, and the whole mixture was further stirred at 60 °C for 10 min with a stirring speed of 600 rpm for uniform mixing. Next, the homogenized mixture was degassed at 60 °C under vacuum for 10–15 min to remove air bubbles. After degassing, the ADC-modified epoxy resin was poured into a mold and subsequently cured at 350 °F for 4 h as recommended by the epoxy manufacturer for best mechanical properties. For comparison, neat epoxy resin (without

Sustainability **2024**, 16, 6870 4 of 14

any ADC particles) was cured with the same curing agent (EPIKURE W) as a control under the same conditions.

2.4. Characterization

The morphology of ADC particles and fracture surfaces of ADC-reinforced EMCs was examined using a Zeiss Auriga Crossbeam FIB Field Emission Scanning Electron Microscope (FESEM, White Plains, NY, USA). Prior to SEM examination, all the samples were sputter-coated with gold-palladium in a thickness of 10 nm to avoid charging. The average size of ADC particles was determined by measuring diameters of at least 50 randomly chosen ADC particles from SEM images using Image J software (version 1.53e). FTIR spectroscopy was performed to identify surface functional groups that were present in ADC particles using an Agilent (Santa Clara, CA, USA) Varian 670 FTIR spectrometer. FTIR spectra were recorded in the wavenumber range of 500 to 4500 cm⁻¹ with 64 scans at room temperature. The surface elements and composition of ADC particles were characterized by X-ray photoelectron spectroscopy (XPS) analysis using a Thermo Scientific (Waltham, MA, USA) Escalab Xi+ XPS instrument. The Advantage software (Version V5.9925) was utilized for XPS data processing, and a combination of Gaussian-Lorentz equations was employed to accurately fit the XPS peaks. To account for charge effect, the binding energy values were calibrated using a reference binding energy of 284.8 eV for C_{1s} (C-C). The surface area and porosity information of the raw and sonicated ADC particles were acquired using nitrogen adsorption through a Micromeritics (Norcross, GA, USA) ASAP 2020 system after the particles were degassed for 4 h. Brunauer-Emmett-Teller (BET) and Barrett-Joyner-Halenda (BJH) models were employed to determine the specific surface area, pore volume, and pore size distribution of ADC particles. The hydrodynamic diameters of raw and sonicated ADC particles were measured using a dynamic light scattering (DLS) technique through a Malvern (Westborough, MA, USA) Zetasizer nano-range instrument. For each sample measurement, 0.1 mg ADC particles were first dispersed in 1 L deionized water and sonicated for 5 min. Following sonication, 1 mL of the obtained dispersion was used for the DLS analysis.

The mechanical properties of the fabricated EMCs were assessed through tensile, flexural (three-point bending), and Izod impact tests at room temperature. Specimens for the respective mechanical test were cut from the prepared EMC panels using a water jet cutting machine (Flow (Kent, WA, USA) MACH 2) in compliance with corresponding ASTM standards. Tensile and flexural tests were carried out on a universal testing machine (UTM Instron (Norwood, MA, USA) 3384) according to ASTM D638-Type IV and ASTM D790, respectively. The Izod impact test was performed on a Tinius Olsen (Horsham, PA, USA) impact tester (Impact 503) following ASTM D256. There were five runs for each EMC sample in each test. The mean value and the associated standard deviation of each sample's test result were reported.

Thermal stability of the ADC-reinforced EMCs was characterized using a Q500 thermogravimetric analyzer (TGA, TA Instruments, New Castle, DE, USA). To identify the effect of ADC particles on thermal stability of the resulting EMCs, ~10 mg of each EMC sample was heated from room temperature to 800 °C with a heating rate of 10 °C/min in a nitrogen gas flow with a flow rate of 50 mL/min while the weight loss of sample against temperature was recorded. This test aimed to assess the thermal degradation behavior of corresponding EMCs. For comparison, TGA analysis of neat epoxy was conducted under the same condition.

3. Results and Discussion

3.1. Characterization of ADC Particles

The diameters of ADC particles from HTL processing of the microalgae varied from \sim 50 nm to \sim 850 nm with an average size of 205 \pm 155 nm (Figure 2A,B). Agglomeration of ADC particles was also observed on SEM images. Submicron ADC particles could form agglomerates that fell into the micrometer range. Consequently, breaking down ADC

Sustainability **2024**, 16, 6870 5 of 14

agglomerates became crucial for ADC particles' application in EMCs. Probe sonication for 30 min at 80% power (400 W) could break the ADC agglomerates and reduced the average size of ADC particles to 136 \pm 74 nm (Figure 2C).

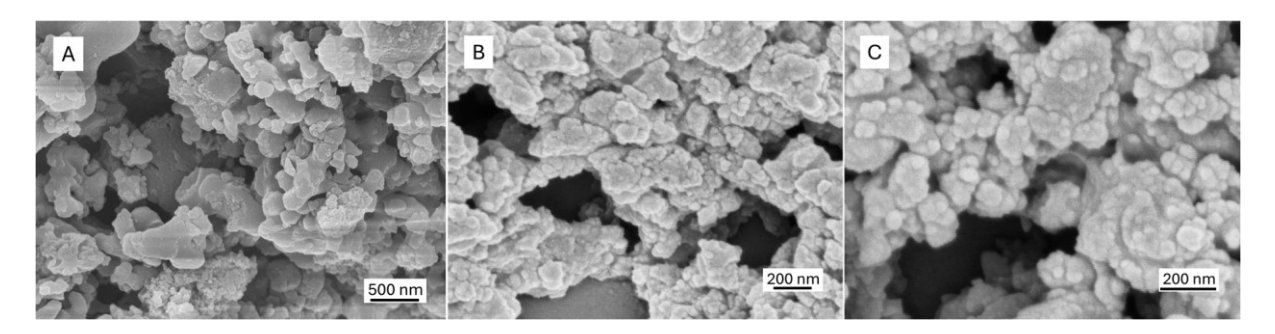


Figure 2. SEM images of raw ADC particles at low **(A)** and high **(B)** magnifications and ADC particles after ultrasonication **(C)**.

DLS was further used to characterize the size of ADC particles. The average size of raw ADC particles was measured to be 722 nm. Following sonication, the average size of ADC particles was notably reduced to 437 nm. In DLS, the measured diameter refers to the hydrodynamic diameter, which represents the size of particles in a solution when accounting for their movement due to Brownian motion. The obtained hydrodynamic diameter of ADC particles was not their actual diameter but rather reflected their effective size as they interacted with surrounding solvent molecules. No matter what, DLS measurements confirmed that sonication is a powerful method to break up agglomerates and reduce the size of ADC particles.

BET surface area analysis was performed to characterize the surface area and porosity of ADC particles. Sonication at 80% power for 30 min induced notable alterations in specific surface area, pore volume, and pore size distribution of ADC particles. The sonication led to a substantial increment in the specific surface area of ADC particles, an improvement of 26 times from \sim 5 m²/g to \sim 130 m²/g. Moreover, sonication resulted in a significant increment in the total pore volume of ADC particles from 0.02349 cm³/g to 0.1963 cm³/g, i.e., an increase of more than 8 times. Additionally, the average pore size of ADC particles decreased significantly from 33 nm to 8.8 nm after sonication.

FTIR was carried out to determine the functional groups in ADC particles (Figure 3A). A broad peak between 3100 and 3600 cm $^{-1}$ in the FTIR spectrum of ADC particles indicated O-H and N-H stretching vibrations, suggesting the presence of hydroxyl and amine functional groups. The FTIR peaks observed in the range of 2800 and 3000 cm $^{-1}$ as well as those around 1450 and 1375 cm $^{-1}$ could represent aliphatic C-H vibrations, while the peaks in the range of 2000 and 1800 cm $^{-1}$ could be assigned to aromatic combination bands. The strong and broad peak between 1800 and 1500 cm $^{-1}$ could be attributed to multiple functional groups including carbonyl, aromatic ring, and amide. The peaks in between 1000 and 1100 cm $^{-1}$ could be ascribed to C-O and C-N stretching vibrations.

Raman spectroscopy serves as a crucial tool for identifying structure defects in a carbon sample. The D band (~1340 cm $^{-1}$) represents the sp^2 carbon hybridized structure, while the G band (~1585 cm $^{-1}$) represents the sp^3 carbon hybridized structure. The intensity ratio of I_D/I_G generally represents the degree of graphitization of carbon materials. The ADC's Raman spectrum (Figure 3B) exhibited both used D band and used G band. The I_D/I_G was found to be 0.61 for ADC particles, indicating both amorphous and ordered carbon structures in these particles.

Sustainability **2024**, 16, 6870 6 of 14

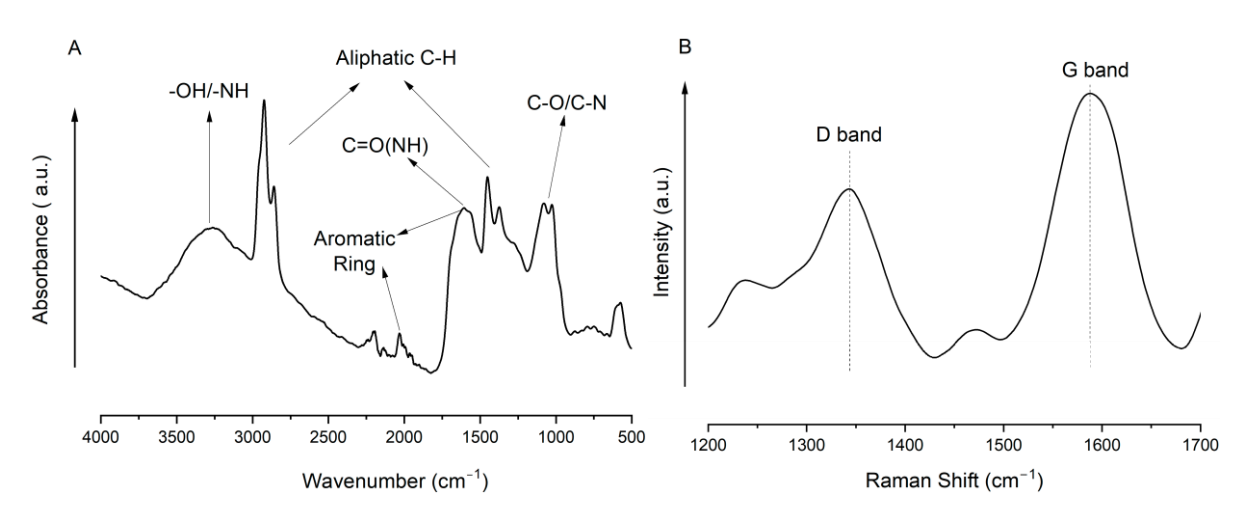


Figure 3. FTIR (A) and Raman (B) spectra of ADC particles.

X-ray photoelectron spectroscopy (XPS) analysis was used to examine ADC particles' surface bonding and elemental composition. The XPS survey (Figure 4A) revealed that the ADC particles had a high carbon content of 82.7%, with nitrogen and oxygen contents being 7.5% and 9.8%, respectively. The ADC's high resolution C_{1s} spectrum (Figure 4B) could be deconvoluted to three distinct peaks at 284.8 eV, 286.1 eV, and 288.8 eV, respectively, corresponding to C-H/C-C, C-O/C-N, and O-C=O/N-C=O [27].

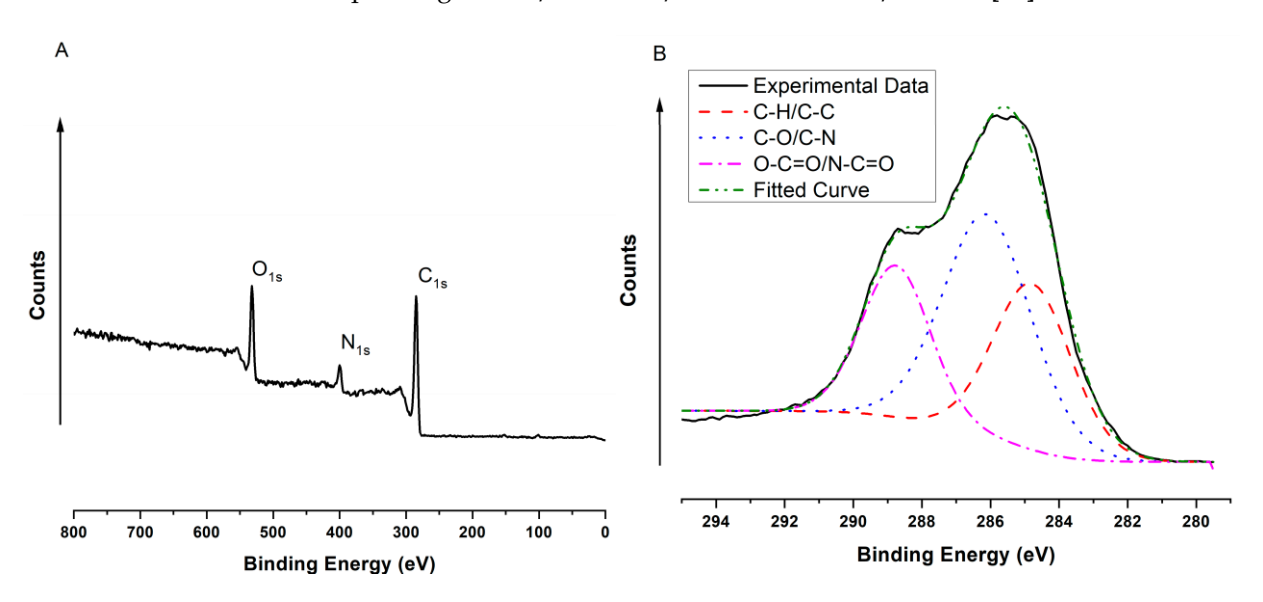


Figure 4. Full survey (A) and high-resolution C1s (B) XPS spectra of ADC particles.

3.2. Reinforcing Effect of ADC Particles

ADC particles sonicated at 80% power for 30 min were employed as a reinforcing agent in EMCs due to their increased surface area and pore volume, which could provide better interaction with the epoxy resin matrix. These ADC particles were dispersed within the epoxy resin matrix at loadings of 0.25%, 0.5%, 1%, and 2% by weight with respect to the total weight of the respective EMC to evaluate their reinforcing effects on the mechanical characteristics of the resulting EMCs. The neat epoxy resin without any filler was cured and tested as a control sample.

3.2.1. Tensile Properties

A tensile test was carried out to determine the mechanical performance of the ADC-reinforced EMCs under uniaxial stretching including tensile strength, Young's modulus, elongation at break, and work of fracture (Figure 5).

Sustainability **2024**, 16, 6870 7 of 14

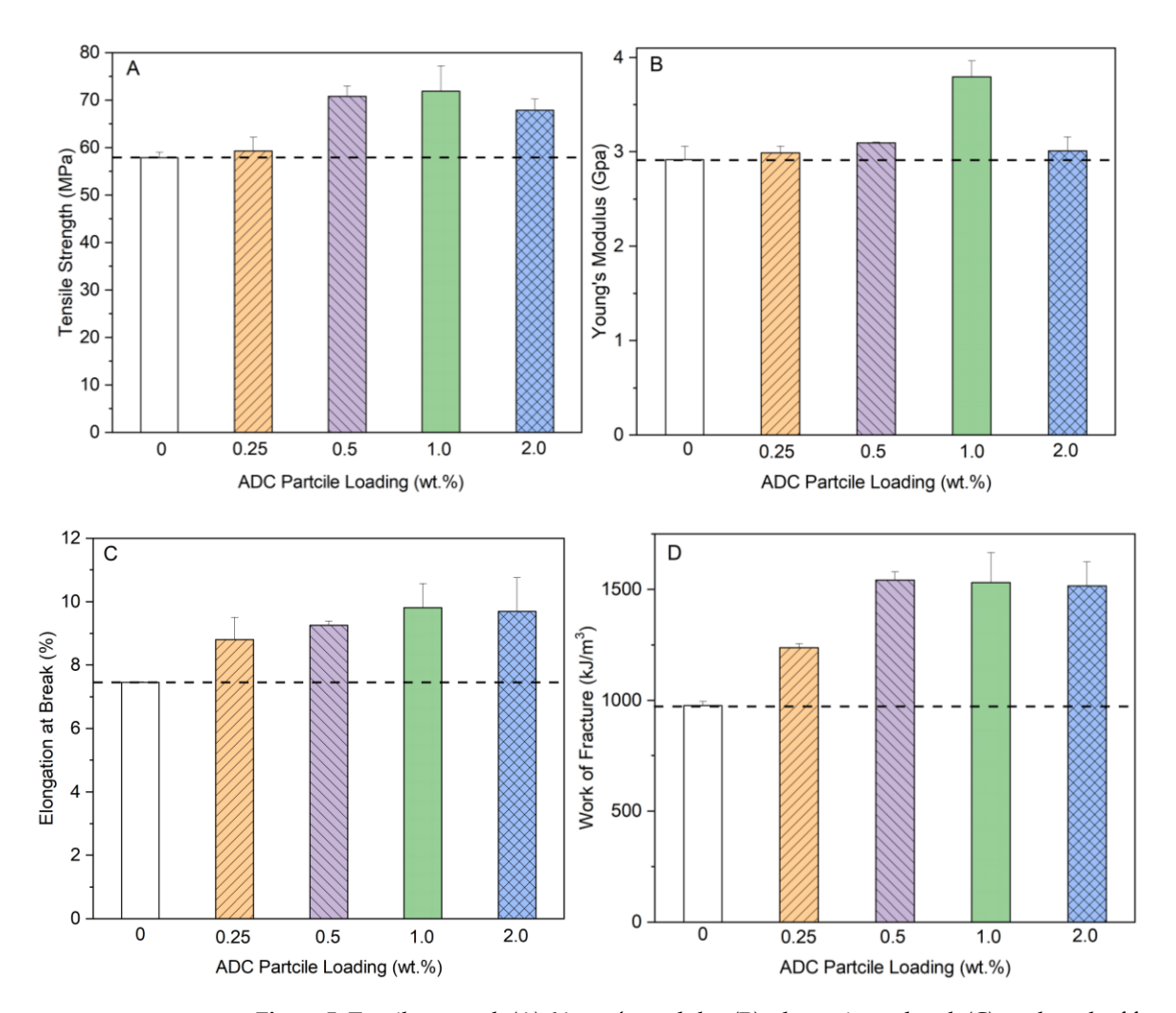


Figure 5. Tensile strength (**A**), Young's modulus (**B**), elongation at break (**C**), and work of fracture (**D**) of neat epoxy resin (control sample) and ADC-reinforced EMCs with ADC particles at loadings of 0.25 wt.%, 0.5 wt.%, 1 wt.%, and 2 wt.% from tensile test.

Tensile strength denotes the maximum tensile stress that a material can withstand before failure. It measures the material's capability to resist breaking under tension. The integration of ADC particles within epoxy resin was observed to have a notable influence on the tensile strength of the resulting EMCs (Figure 5A). Compared to the tensile strength of neat epoxy resin (57.9 MPa), incorporating ADC particles resulted in a slight tensile strength improvement of \sim 3% at 0.25 wt.% loading, and a substantial improvement of \sim 22% at 0.5 wt.% loading. The EMC containing 1 wt.% ADC particles demonstrated the maximum tensile strength with a \sim 24% increment over that of the neat epoxy. However, further increasing the ADC particle loading to 2 wt.% resulted in a drop of tensile strength.

Young's modulus is an indicator of a material's stiffness, quantifying its resistance to elastic deformation under applied tensile stress. ADC particles exhibited a notable effect on the stiffness of the resultant epoxy composites (Figure 5B). Compared to the neat epoxy's modulus of 2.91 GPa, the inclusion of ADC particles resulted in a modulus range between 2.98 and 3.79 GPa. The highest modulus was observed with 1 wt.% ADC particle loading, which showed a \sim 30% improvement over the neat epoxy.

Elongation at break measures a material's stretchability before failure, indicating ductility. Its significance lies in assessing the material's flexibility and resilience under stress. All the ADC-reinforced EMCs showed significant improvement in elongation at break (Figure 5C). Among all ADC-reinforced EMCs, the EMC with 1 wt.% ADC particles

Sustainability **2024**, 16, 6870 8 of 14

exhibited the maximum enhancement of elongation at break, i.e., ~31% improvement compared to that of neat epoxy.

Work of fracture (WOF) in a tensile test quantifies the energy absorbed by the testing sample before failure, indicating its static toughness. It is essential for assessing materials' resistance to tensile loading, showing their durability. The WOF herein was quantified by the area under the sample's stress–strain curve. It is noteworthy that the inclusion of ADC particles drastically improved the WOF of EMCs (Figure 5D). The WOFs of EMCs with 0.25 wt.%, 0.5 wt.%, 1 wt.%, and 2 wt.% ADC particles were improved by ~27%, ~58%, ~57%, and ~55%, respectively, compared to neat epoxy.

Overall, ADC particles demonstrated both reinforcing and toughening effects on the EMCs. Particularly, incorporation of 1 wt.% ADC particles in the epoxy resin achieved the most significant improvement in tensile strength, stiffness, ductility, and toughness by \sim 24%, \sim 30%, \sim 31%, and \sim 57%, respectively.

3.2.2. Flexural Properties

A flexural test was performed to analyze ADC-reinforced EMCs' ability to resist bending load. Flexural properties of the ADC-reinforced EMCs, including flexural strength, modulus, elongation at break, and work of fracture, were investigated (Figure 6).

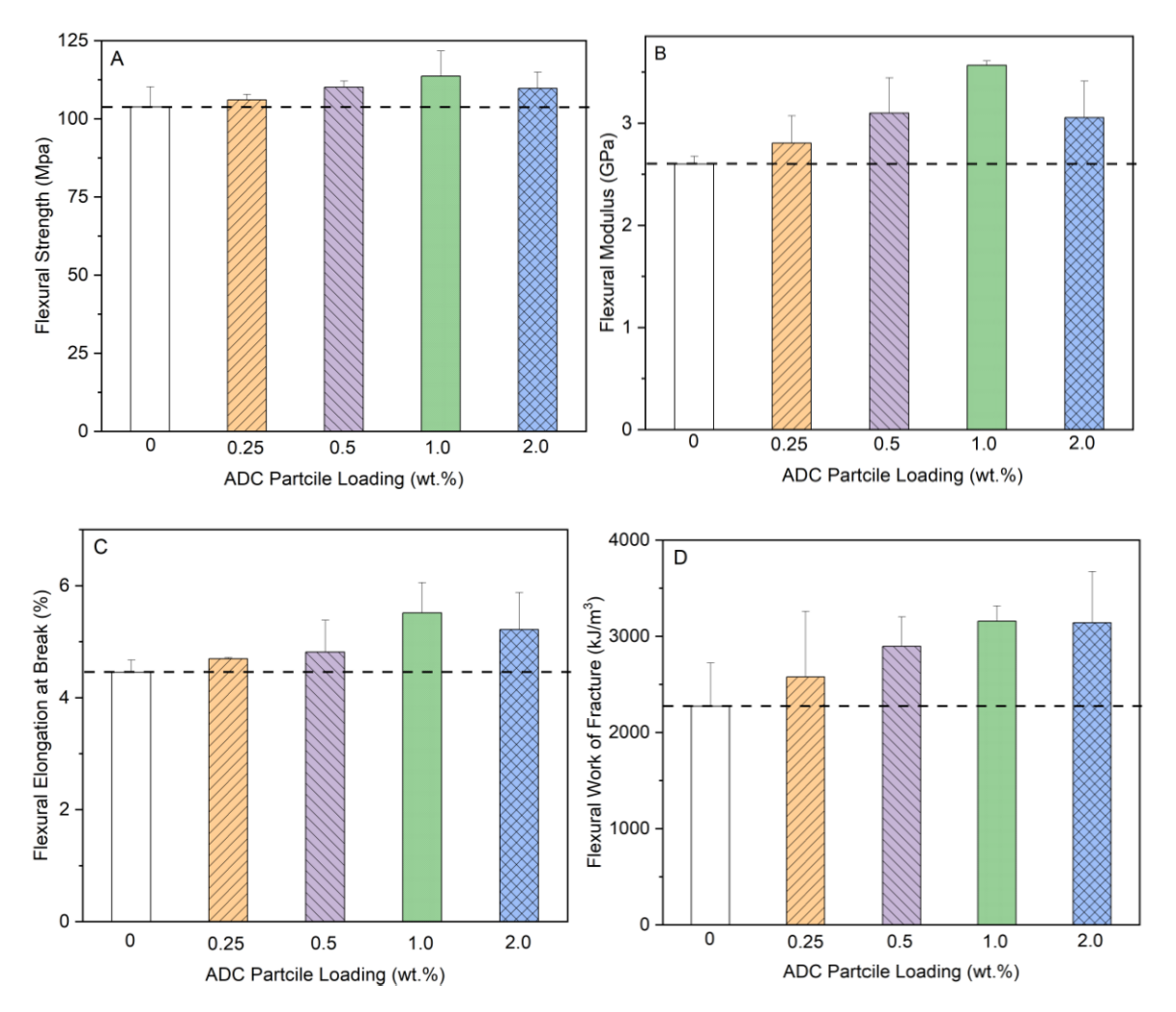


Figure 6. Flexural strength (**A**), flexural modulus (**B**), flexural elongation at break (**C**), and flexural work of fracture (**D**) of neat epoxy resin (control sample) and ADC-reinforced EMCs with ADC particle loadings at 0.25 wt.%, 0.5 wt.%, 1 wt.%, and 2 wt.% from the flexural (three-point bending) test.

Sustainability **2024**, 16, 6870 9 of 14

Flexural strength refers to the maximum stress that a material can withstand before breaking when subjected to a bending load. The flexural strength of ADC-reinforced EMCs was barely affected by incorporation of ADC particles at a low loading of 0.25 wt.% (Figure 6A). A slight improvement of \sim 6% in flexural strength of the EMC was observed at 0.5 wt.% loading of ADC particles. The ADC-reinforced EMC at 1 wt.% ADC loading exhibited the maximum improvement in flexural strength, i.e., \sim 10% improvement compared to that of neat epoxy. Further increasing ADC loading resulted in less improvement in flexural strength. Only \sim 5% improvement in flexural strength of the EMC was observed at higher ADC particle loading of 2 wt.%.

Flexural modulus measures a material's rigidity against bending force, which is determined by the stress-to-strain ratio in the elastic region of a flexural test. It reflects the material's ability to resist bending deformation. The flexural modulus of the neat epoxy sample was 2.59 GPa, and the incorporation of ADC particles led to increased flexural moduli in all the resultant EMCs (Figure 6B). The introduction of ADC particles at 0.25 wt.%, 0.5 wt.%, 1 wt.%, and 2 wt.% loadings caused increases in EMCs' flexural stiffness by ~8%, ~19%, ~37%, and ~17%, respectively. Notably, the inclusion of 1 wt.% ADC particles improved the flexural stiffness of the epoxy resin from 2.59 GPa to 3.56 GPa.

Flexural elongation at break quantifies the degree of deformation experienced by a material when it is subjected to bending load. The flexural elongation at break of the neat epoxy was 4.45%. The introduction of ADC particles demonstrated a progressive enhancement in flexural elongation at break of the EMCs across all loading levels and increased the flexural elongation at break by ~5%, ~8%, ~24%, and ~17%, respectively, at ADC loadings of 0.25 wt.%, 0.5 wt.%, 1 wt.%, and 2 wt.%, as shown in Figure 6C.

Flexural work of fracture (WOF) refers to the energy required to fracture a material when it is subjected to a bending load, reflecting its toughness and ability to withstand bending force without failure. The ADC-reinforced EMCs with 0.25 wt.% and 0.5 wt.% ADC loadings demonstrated \sim 13% and \sim 27% enhancement in flexural WOF, respectively, compared to that of the neat epoxy (2272 kJ/m³). In particular, the EMCs containing 1 wt.% and 2 wt.% ADC particles exhibited similar enhancements in flexural WOF, which were the maximum among all the samples, i.e., \sim 39% over the neat epoxy (Figure 6D).

Overall, ADC particles also demonstrated reinforcing and toughening effects on the EMCs from the flexural test. Particularly, incorporation of 1 wt.% of ADC particles in the epoxy resin achieved the most significant improvement in flexural strength, stiffness, ductility, and toughness by $\sim 10\%$, $\sim 37\%$, $\sim 24\%$, and $\sim 39\%$, respectively.

3.2.3. Impact Property

The Izod impact test on notched specimens was carried out to evaluate the toughness (energy absorption capacity) of the ADC-reinforced EMCs when they were subjected to sudden impacts. Figure 7 depicts the energy absorption of ADC-reinforced EMCs with ADC loadings at 0.25 wt.%, 0.5 wt.%, 1 wt.%, and 2 wt.%, respectively, during impact. Compared to the Izod impact strength of neat epoxy (16.6 J/m), incorporation of ADC particles brought about increases in impact strength of the resultant EMCs over all the loading levels in this study. At loadings of 0.25 wt.% and 0.5 wt.%, the addition of ADC particles led to \sim 46% and \sim 51% improvements in Izod impact strength, respectively. The maximum improvement of \sim 54% in Izod impact strength was achieved with the EMC containing 1 wt.% ADC particles. With a further increase in ADC particle loading to 2 wt.%, the Izod impact strength of the EMC fell significantly, though it still exceeded that of the neat epoxy by \sim 17%.

Sustainability **2024**, 16, 6870 10 of 14

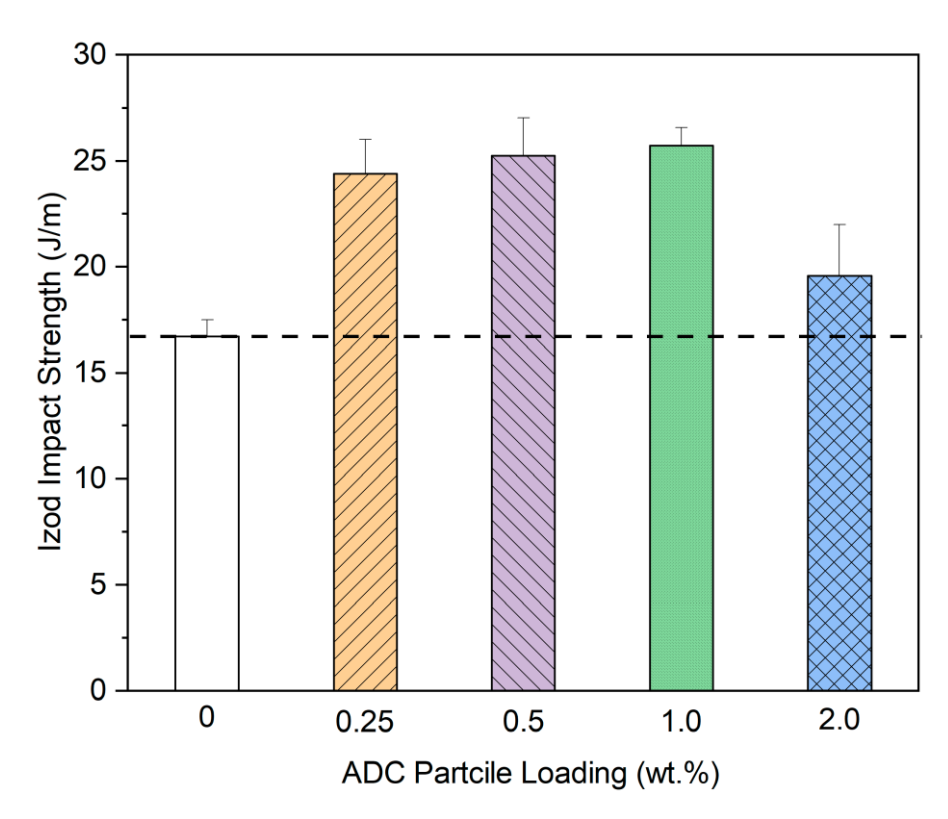


Figure 7. Izod impact strength of neat epoxy resin (control sample) and ADC-reinforced EMCs with ADC particle loadings at 0.25 wt.%, 0.5 wt.%, 1 wt.%, and 2 wt.% from the Izod impact test.

3.3. Discussion on the Reinforcing Mechanism of ADC Particles

To understand the reinforcing mechanism of ADC particles in epoxy matrix, fracture surfaces of the neat epoxy sample and the ADC-reinforced EMC sample with ADC particles at 1 wt.% loading after tensile, flexural, and Izod impact tests were examined using SEM (Figure 8). The fracture surfaces of the neat epoxy sample (Figure 8A1–A3) exhibited smooth texture with few oriented fracture lines. The relatively smooth surface represented less resistance to the applied load and low energy absorption before its failure. In comparison to that of neat epoxy, the fracture surfaces of the ADC-reinforced EMC with 1 wt.% ADC particles (Figure 8B1–B3) showed high surface roughness and multi-plane fracture lines, indicating much more energy consumption than that of the neat epoxy sample upon failure, and correspondingly much higher toughness.

The reinforcing effects of ADC particles in epoxy resin could be attributed to a strong interfacial bonding-enhanced rigid particle reinforcing mechanism. The hydroxyl, carboxyl, and amine functional groups on the surface of the ADC particles could react with epoxide functional groups in epoxy resin. This led to the formation of strong covalent bonds that realized a strong interfacial bonding between the ADC particles and the epoxy matrix. In addition, the small size, high specific surface area, and large pore volume of ADC particles further strengthened the interfacial bonding between ADC particles and epoxy matrix. The robust interfacial bonding in ADC-reinforced EMCs resulted in more efficient stress transfer and distribution within the epoxy matrix as well as mechanical interlocking and greater energy absorption in the case of debonding. When the ADC-reinforced EMCs were subjected to external loading force, microcracks could form in the epoxy matrix due to high local stress concentration and then propagate through the matrix. When the microcracks encountered ADC particles, the rigid particles could bridge the crack faces and stop microcracks' propagation. When the applied load exceeded the interfacial bonding strength, debonding of ADC particles would occur [28,29]. The crack bridging effect from rigid ADC particles as well as the large energy consumption to partially/completely debond the ADC particles from the epoxy matrix due to the strong interfacial bonding

Sustainability **2024**, 16, 6870

would increase the epoxy matrix's resistance to crack growth and improve its mechanical performance (Figure 9).

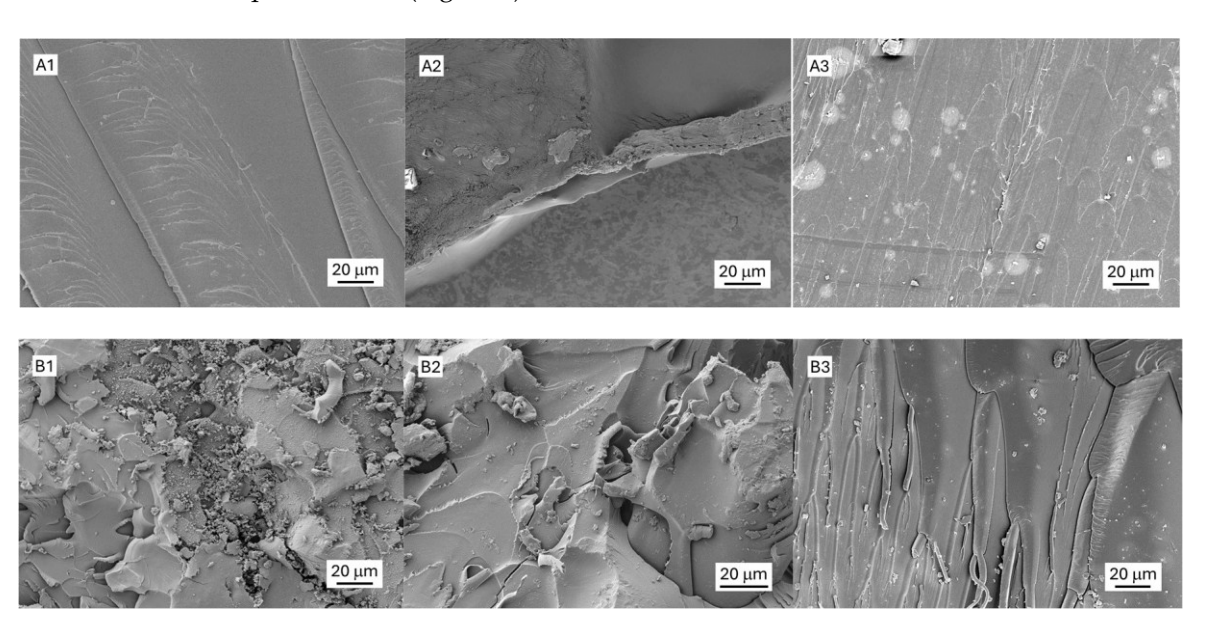


Figure 8. Representative SEM images of fracture surfaces of neat epoxy (**A**) and the ADC-reinforced EMC with ADC loading of 1 wt.% (**B**) after mechanical tests. Labels "1", "2", and "3" stand for tensile test, flexural test, and Izod impact test, respectively.

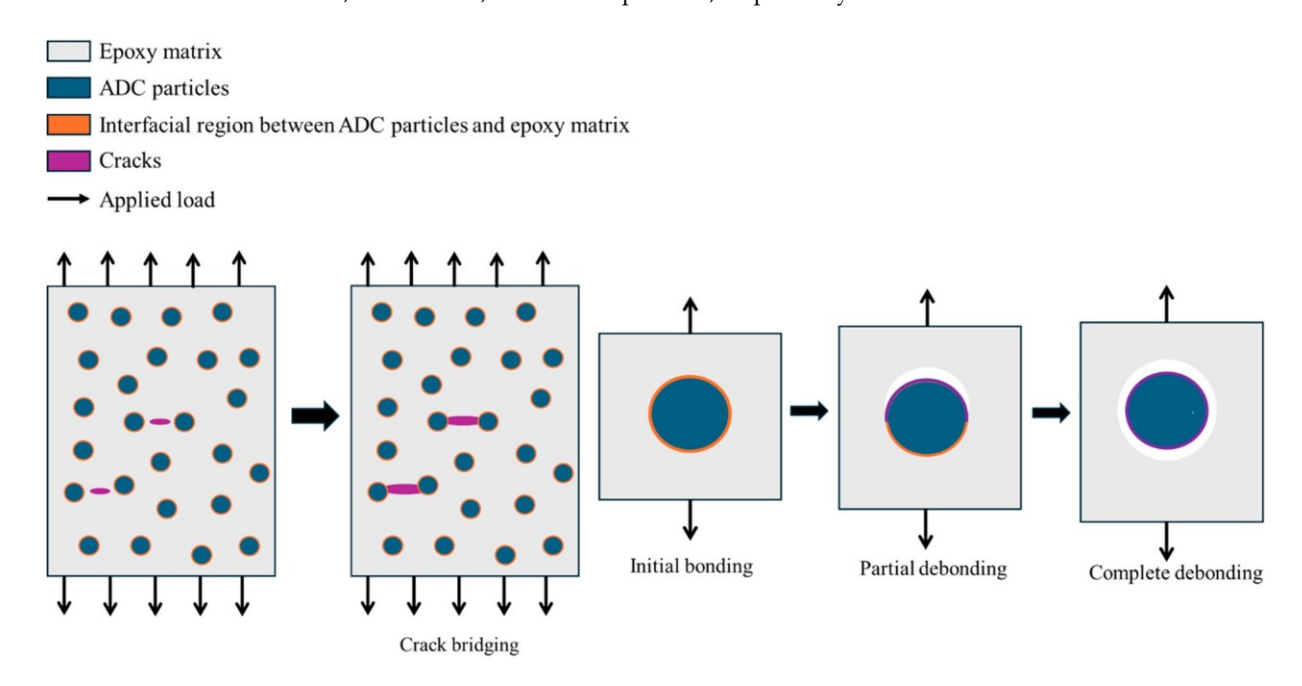


Figure 9. Schematic diagram of the strong interfacial bonding-enhanced rigid particle reinforcing mechanism of ADC particles in ADC-reinforced EMCs.

It is noteworthy that high loadings of ADC particles in EMCs (e.g., 2 wt.%) could result in agglomeration of ADC particles in the epoxy matrix. The agglomerates of ADC particles then became defective sites instead of reinforcing sites and gave rise to the degradation of mechanical performance of the resultant EMCs.

3.4. Thermal Stability of ADC-Reinforced EMCs

To evaluate the thermal stability of ADC-reinforced EMCs, thermogravimetric analysis (TGA) was performed. The respective decomposition temperatures of the ADC-reinforced

Sustainability **2024**, 16, 6870 12 of 14

EMCs with ADC particle loadings at 0.25 wt.%, 0.5 wt.%, 1 wt.%, and 2 wt.% corresponding to 10%, 20%, 60%, and 80% weight loss were revealed (Figure 10).

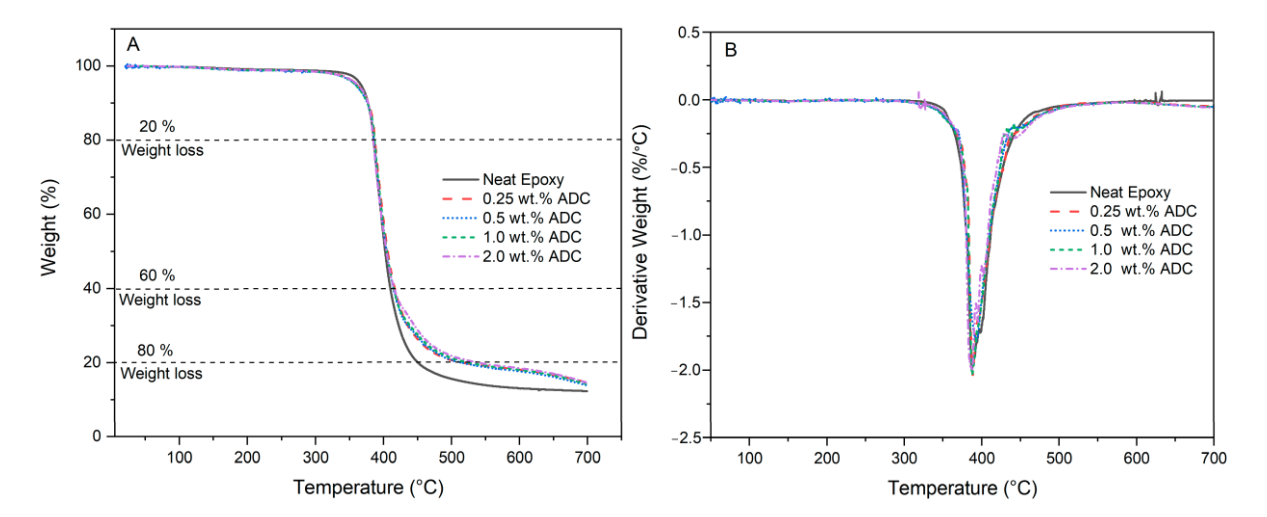


Figure 10. Typical weight loss (**A**) and the derivative weight loss (**B**) against temperature of neat epoxy (control sample) and ADC-reinforced EMCs with ADC loading levels at 0.25 wt.%, 0.5 wt.%, 1 wt.%, and 2 wt.% from thermogravimetric analysis (TGA).

It was observed that inclusion of ADC particles as reinforcing filler in the epoxy resin improved its thermal stability (Figure 10A). The addition of ADC particles improved the decomposition temperature at 60% weight loss of all the studied EMC samples at similar levels, which increased from 410 °C for the neat epoxy to 415 °C for the ADC-reinforced EMCs. More significant increases in the decomposition temperature at 80% weight loss were observed for all the studied ADC-reinforced EMCs and the temperature increased with ADC loading. The highest decomposition temperature at 80% weight loss of the EMCs was observed with 2 wt.% ADC, which increased from 448 °C for neat epoxy to 527 °C. The derivative thermogravimetric (DTG) analysis (Figure 10B) showed no significant change in the maximum rate of degradation among all the ADC-reinforced EMCs.

The improvements of thermal stability of the ADC-reinforced EMCs could be assigned to (1) the high carbon content of ADC particles, which are thermally stable; (2) the high interfacial bonding between ADC particles and epoxy matrix, which caused more thermal energy to break all the bonds between the ADC particles and the epoxy matrix.

4. Conclusions

This research highlighted the potential of algae-derived carbon (ADC) particles, a byproduct generated in the process of hydrothermal liquefaction (HTL) of microalgae for bio-crude oil production, as an innovative reinforcing agent for polymer composites. The as-generated ADC particles from HTL of Chlorella vulgaris (a green microalgae) exhibited an average size of ~205 nm, while ultrasonication could break ADC agglomerates and increased their specific surface area from ~5 m²/g to ~130 m²/g. Integration of ADC particles into epoxy resin (EPON 862) from 0.25 wt. % up to 2 wt. % enhanced the mechanical properties of the resulting epoxy matrix composites (EMCs) with the maximum mechanical performance observed at 1 wt.% ADC particle loading. Compared to the neat epoxy, the incorporation of 1 wt.% ADC particles significantly improved the tensile strength, Young's modulus, elongation at break, and work of fracture (WOF) of the EMC by ~24%, ~30%, ~31%, and ~57%, respectively, and the flexural strength, flexural modulus, flexural elongation at break, and flexural WOF of the EMC by ~10%, ~37%, ~24%, and ~39%, respectively. Moreover, the Izod impact strength of the EMC with 1 wt.% ADC particles increased by ~54% with respect to that of the neat epoxy. Inclusion of ADC particles in the epoxy resin also enhanced its thermal stability. Significantly higher decomposition temperatures at 60% and 80% weight loss were observed for all the studied ADC-reinforced

Sustainability **2024**, 16, 6870

EMCs as compared to those of neat epoxy. The reinforcing effect of ADC particles in epoxy matrix could be attributed to a strong interfacial bonding-enhanced rigid particle reinforcing mechanism. The ADC particles with intrinsically developed abundant surface functional groups such as amine, hydroxyl, carboxylic acid, amide, and aromatic rings as well as small size, ample specific surface area, and large pore volume from HTL processing of the microalgae could effectively bond with epoxy matrix to enhance the interfacial bonding in the resultant ADC-reinforced EMCs. The crack bridging effect by rigid ADC particles, as well as the large energy consumption caused by the debonding of ADC particles from epoxy matrix due to strong interfacial bonding, resulted in significant improvement in mechanical performance. Overall, the byproduct of ADC particles from HTL of microalgae stand out as a promising reinforcing agent in polymer composite materials. This novel application of ADC particles contributed to the broader goals of sustainable development and offers an eco-friendly alternative to conventional non-renewable fillers.

Author Contributions: Conceptualization, L.W. and L.Z.; methodology, A.M., V.S.J., L.W. and L.Z.; validation, A.M., P.A., S.M. and V.S.J.; formal analysis, A.M.; investigation, A.M., P.A. and S.M.; resources, L.W. and L.Z.; writing—original draft preparation, A.M.; writing—review and editing, L.Z.; supervision, L.W. and L.Z.; project administration, L.Z.; funding acquisition, L.Z. All authors have read and agreed to the published version of the manuscript.

Funding: This research was funded by the National Science Foundation (CMMI 2000318).

Institutional Review Board Statement: Not applicable.

Informed Consent Statement: Not applicable.

Data Availability Statement: Data are contained within the article. The original contributions presented in this study are included in the article; further inquiries can be directed to the corresponding author/s.

Acknowledgments: This work was conducted at the Joint School of Nanoscience and Nanoengineering of North Carolina A&T State University, a member of the Southeastern Nanotechnology Infrastructure Corridor (SENIC) and National Nanotechnology Coordinated Infrastructure (NNCI), which is supported by the National Science Foundation (ECCS-2025462).

Conflicts of Interest: The authors declare no conflicts of interest.

References

- 1. May, C.A. Epoxy Resins: Chemistry and Technology, 2nd ed.; Marcel Dekker: New York, NY, USA, 1988; p. 1.
- 2. Tee, Z.Y.; Yeap, S.P.; Hassan, C.S.; Kiew, P.L. Nano and non-nano fillers in enhancing mechanical properties of epoxy resins: A brief review. *Polym. Plast. Technol. Mater.* **2022**, *61*, 709–725. [CrossRef]
- 3. Karnati, S.R.; Agbo, P.; Zhang, L. Applications of silica nanoparticles in glass/carbon fiber-reinforced epoxy nanocomposite. *Compos. Commun.* **2020**, *17*, 32–41. [CrossRef]
- 4. Matykiewicz, D. Hybrid epoxy composites with both powder and fiber filler: A Review of Mechanical and Thermomechanical Properties. *Materials* **2020**, *13*, 1802. [CrossRef]
- 5. Bello, S.A.; Agunsoye, J.O.; Hassan, S.B.; Kana, M.G.Z.; Raheem, I.A. Epoxy resin-based composites, mechanical and tribological properties: A review. *Tribol. Ind.* **2015**, *37*, 500–524.
- 6. Mali, A.; Agbo, P.; Mantripragada, S.; Zhang, L. Surface-modified electrospun glass nanofibers from silane treatment and their use for high-performance epoxy-based nanocomposite materials. *Materials* **2023**, *16*, 6817. [CrossRef] [PubMed]
- 7. Prashanth, S.; Subbaya, K.M.; Nithin, K.; Sachhidananda, S. Fiber reinforced composites A review. *J. Mater. Sci. Eng.* **2017**, *6*, 341. [CrossRef]
- 8. Bilyeu, B.; Brostow, W.; Menard, K.P. Epoxy thermosets and their applications I: Chemical structures and applications. *J. Mater. Educ.* **1999**, 21, 281–286.
- 9. Zhao, Q.; Hoa, S.V. Toughening mechanism of epoxy resins with micro/nano particles. *J. Compos. Mater.* **2007**, 41, 201–219. [CrossRef]
- 10. Garg, A.C.; Mai, Y.-W. Failure mechanisms in toughened epoxy resins—A review. *Compos. Sci. Technol.* **1988**, 31, 179–223. [CrossRef]
- 11. Moloney, A.C.; Kausch, H.H.; Stieger, H.R. The fracture of particulate-filled epoxide resins. *J. Mater. Sci.* **1983**, *18*, 208–216. [CrossRef]

Sustainability **2024**, 16, 6870 14 of 14

12. Zunjarrao, S.C.; Singh, R.P. Characterization of the fracture behavior of epoxy reinforced with nanometer and micrometer sized aluminum particles. *Compos. Sci. Technol.* **2006**, *66*, 2296–2305. [CrossRef]

- 13. Singh, S.K.; Singh, S.; Kumar, A.; Jain, A. Thermo-mechanical behavior of TiO₂ dispersed epoxy composites. *Eng. Fract. Mech.* **2017**, *184*, 241–248. [CrossRef]
- 14. Sanya, O.T.; Oji, B.; Owoeye, S.S.; Egbochie, E.J. Influence of particle size and particle loading on mechanical properties of silicon carbide-reinforced epoxy composites. *Int. J. Adv. Manuf. Technol.* **2019**, *103*, 4787-4794. [CrossRef]
- 15. Misiura, A.I.; Mamunya, Y.P.; Kulish, M.P. Metal-filled epoxy composites: Mechanical properties and electrical/thermal conductivity. *J. Macromol. Sci. Part B* **2019**, *59*, 121–136. [CrossRef]
- 16. La Mantia, F.P.; Morreale, M. Green composites: A brief review. Compos. Part A Appl. Sci. Manuf. 2011, 42, 579–588. [CrossRef]
- 17. Aup-Ngoen, K.; Noipitak, M. Effect of carbon-rich biochar on mechanical properties of PLA-biochar composites. *Sustain. Chem. Pharm.* **2020**, *15*, 100204. [CrossRef]
- 18. Das, C.; Tamrakar, S.; Kiziltas, A.; Xie, X. Incorporation of biochar to improve mechanical, thermal and electrical properties of polymer composites. *Polymers* **2021**, *13*, 2663. [CrossRef] [PubMed]
- 19. Das, O.; Bhattacharyya, D.; Hui, D.; Lau, K.T. Mechanical and flammability characterizations of biochar/polypropylene biocomposites. *Compos. Part B* **2016**, *106*, 120–128. [CrossRef]
- 20. Nizamuddin, S.; Hossain, N.; Qureshi, S.S.; Al-Mohaimeed, A.M.; Tanjung, F.A.; Elshikh, M.S.; Siddiqui, M.T.H.; Baloch, H.A.; Mubarak, N.M.; Griffin, G.; et al. Experimental investigation of physicochemical, thermal, mechanical and rheological properties of polylactide/rice straw hydrochar composite. *J. Environ. Chem. Eng.* **2021**, *9*, 106011. [CrossRef]
- 21. Zhang, Q.; Xu, H.; Lu, W.; Zhang, D.; Ren, X.; Yu, W.; Wu, J.; Zhou, L.; Han, X.; Yi, W.; et al. Properties evaluation of biochar/high-density polyethylene composites: Emphasizing the porous structure of biochar by activation. *Sci. Total Environ.* **2020**, 737, 139770. [CrossRef]
- 22. Gollakota, A.R.K.; Kishore, N.; Gu, S. A review on hydrothermal liquefaction of biomass. *Renew. Sustain. Energy Rev.* **2018**, 81, 1378–1392. [CrossRef]
- 23. Agbo, P.; Mali, A.; Deng, D.; Zhang, L. Bio-oil-based epoxy resins from thermochemical processing of sustainable resources: A short review. *J. Compos. Sci.* **2023**, *7*, 374. [CrossRef]
- 24. Tian, C.; Li, B.; Liu, Z.; Zhang, Y.; Lu, H. Hydrothermal liquefaction for algal biorefinery: A critical review. *Renew. Sustain. Energy Rev.* **2014**, *38*, 933–950. [CrossRef]
- 25. Guo, Y.; Yeh, T.; Song, W.; Xu, D.; Wang, S. A review of bio-oil production from hydrothermal liquefaction of algae. *Renew. Sustain. Energy Rev.* **2015**, *48*, 776–790. [CrossRef]
- 26. Agbo, P.; Mali, A.; Kelkar, A.D.; Wang, L.; Zhang, L. Injecting sustainability into epoxy-based composite materials by using bio-binder from hydrothermal liquefaction processing of microalgae. *Molecules* **2024**, *29*, 3656. [CrossRef]
- 27. Mantripragada, S.; Dong, M.; Zhang, L. Sustainable filter/adsorbent materials from cellulose-based nanofibrous membranes with soy protein coating for high-efficiency GenX fluorocarbon remediation from water. *Cellulose* **2023**, *30*, 7063–7078. [CrossRef]
- 28. Anderson, T.L. Fracture Mechanics: Fundamentals and Applications, 4th ed.; CRC Press: Boca Raton, FL, USA, 2017.
- Meng, Q.; Wang, T. An improved crack-bridging model for rigid particle-polymer composites. Eng. Fract. Mech. 2019, 211, 291–302.
 [CrossRef]

Disclaimer/Publisher's Note: The statements, opinions and data contained in all publications are solely those of the individual author(s) and contributor(s) and not of MDPI and/or the editor(s). MDPI and/or the editor(s) disclaim responsibility for any injury to people or property resulting from any ideas, methods, instructions or products referred to in the content.